Sensitivity of Easterly QBO's Boreal Winter Teleconnections and Surface Impacts to SSWs

DILLON ELSBURY,[a,b] AMY BUTLER,[b] YANNICK PEINGS,[c] AND GUDRUN MAGNUSDOTTIR[c]

[a] *Cooperative Institute for Research in Environmental Sciences, University of Colorado Boulder, Boulder, Colorado*
[b] *NOAA/Chemical Sciences Laboratory, Boulder, Colorado*
[c] *Department of Earth System Science, University of California, Irvine, Irvine, California*

(Manuscript received 1 July 2023, in final form 23 February 2024, accepted 11 March 2024)

ABSTRACT: The quasi-biennial oscillation (QBO) is thought to influence boreal winter surface conditions over Asia and around the North Atlantic. Confirming if these responses are robust is complicated by the QBO having multiple pathways to influence surface conditions as well as internal variability. The reanalysis record suggests that sudden stratospheric warmings (SSWs), breakdowns of the polar vortex that can elicit persistent surface impacts, are more frequent during easterly QBO (EQBO). Hence, this modulated frequency of SSWs may account for some of the EQBO surface responses. However, many climate models do not reproduce this QBO–SSW relationship, perhaps because it is noise or because the model QBOs are deficient. We circumvent these issues by using an ensemble of fixed boundary condition branched simulations in which a realistic EQBO is prescribed in control simulations previously devoid of a QBO, allowing us to isolate the transient atmospheric response to EQBO. Imposing EQBO accelerates the tropical upper-tropospheric wind, shifts the subtropical jet poleward, and attenuates the polar vortex. Interestingly, the latter is not entirely dependent on the statistically significant increase in SSW frequency due to EQBO. Corroborating observations, EQBO is associated with warmer surface temperatures over Asia and negative North Atlantic Oscillation (NAO) conditions. We then subsample the branched/control simulations based on which EQBO members have SSWs. The negative NAO response is primarily associated with more frequent SSWs, while the Asia warming develops irrespective of SSWs. These results have implications for wintertime predictability and clarify the pairing of particular QBO teleconnections with certain surface impacts.

SIGNIFICANCE STATEMENT: The QBO is one of the few parts of the Earth system that is predictable months in advance and that also elicits global effects on surface temperature, circulation, and precipitation. Unfortunately, climate models and operational forecast systems do not simulate the QBO well and it is not always clear how robust the global impacts of the QBO are. Here, we impose the QBO in idealized model simulations, which modulates wintertime surface temperature and precipitation over Asia, the North Atlantic, Europe, and Africa in a manner consistent with observations. This work substantiates the importance of climate and forecast models properly simulating the QBO.

KEYWORDS: Quasi-biennial oscillation; Teleconnections; Surface pressure

1. Introduction

Observational evidence indicates that boreal winter surface conditions fluctuate in response to the quasi-biennial oscillation (QBO). The periodic descending and alternating easterly and westerly winds in the tropical stratosphere that comprise the QBO modify the stratospheric circulation from tropics to pole, which is thought to give rise to tropospheric impacts (Gray et al. 2018). Studies point to the QBO affecting wintertime surface conditions over Asia (Chen and Li 2007; Ma et al. 2021; Zuo et al. 2022; Park et al. 2022) as well as over the landmasses surrounding the North Atlantic (Angell et al. 1969; Anstey and Shepherd 2014; Andrews et al. 2019; O'Reilly et al. 2019; Rao et al. 2020b). Identifying how the QBO interacts with the surface and whether or not these responses are robust is complicated by the QBO having multiple pathways to influence the troposphere and by internal variability.

The QBO interacts with the troposphere through tropical, subtropical, and polar routes (Gray et al. 2018). The tropical route refers to fluctuations in tropical circulation and precipitation location and variability under different phases of the QBO (Liess and Geller 2012; Son et al. 2017; Hitchman et al. 2021). Upper-tropospheric–lower-stratospheric stability (Densmore et al. 2019), cloud radiative processes (Sakaeda et al. 2020), the Walker circulation (García-Franco et al. 2022), the structure of the tropopause (Tegtmeier et al. 2020), as well as the amplitude and propagation speed of the Madden–Julian oscillation (Lim et al. 2019; Martin et al. 2021b) are all impacted by the QBO phase. The QBO's effect on the tropical troposphere also influences poleward Rossby wave propagation through the upper troposphere (Yamazaki et al. 2020), which is a means by which the QBO modifies regional circulation variability over the midlatitudes globally (e.g., Sena et al. 2022). Unfortunately, the tropical route is underestimated in climate models (Rao et al. 2020a; Serva et al. 2022), which could preclude the QBO from eliciting its full range of teleconnections and surface impacts in models.

Supplemental information related to this paper is available at the Journals Online website: https://doi.org/10.1175/JCLI-D-23-0395.s1.

Corresponding author: Dillon Elsbury, dillon.elsbury@noaa.gov

DOI: 10.1175/JCLI-D-23-0395.1

Another pathway by which the QBO's influence extends into the extratropics is through the subtropical route. The QBO winds arch poleward and downward out of the tropics toward the subtropical upper troposphere, weakening the upper-tropospheric zonal-mean zonal winds near 20°N during easterly QBO (EQBO). This zonal wind response is particularly strong near the North Pacific (Wang et al. 2018; Rao et al. 2020a; Elsbury et al. 2021a; Ma et al. 2021: Anstey et al. 2022), although an analogous teleconnection appears to operate over the North Atlantic too (Wang et al. 2018). The subtropical route develops in response to the QBO's mean meridional circulation (QBO-MMC) (Garfinkel and Hartmann 2011a,b), a secondary circulation intrinsically associated with the QBO (Plumb and Bell 1982) whose poleward extent is continuously modified by extratropical wave–mean flow and wave–wave interactions (Inoue and Takahashi 2013; White et al. 2015; Wang et al. 2018; Haynes et al. 2021). The zonal wind anomalies associated with the subtropical route can reach down to Earth's surface (Garfinkel and Hartmann 2011a,b) and are thought to promote surface warming over East Asia during EQBO boreal winters (Ma et al. 2021).

The final pathway the QBO uses to interact with the surface is the polar route via the Holton–Tan effect (Holton and Tan 1980). The QBO modifies the strength and position of the polar vortex, which projects onto the surface North Atlantic Oscillation (Anstey and Shepherd 2014; Zhang et al. 2019). Some CMIP6 models simulate this teleconnection and its associated surface North Atlantic Oscillation (NAO) response, while others do not (Rao et al. 2020a; Elsbury et al. 2021b), with this spread in representation conceivably resulting from the deficient structure of the model QBOs (Hansen et al. 2013; Richter et al. 2020), model circulation biases (Karpechko et al. 2021), or internal variability (Lu et al. 2014; Kumar et al. 2022). There are a range of mechanistic explanations for the Holton–Tan effect. The classic Holton and Tan (1980) mechanism emphasizes that the zero wind line partitioning the QBO easterlies and Northern Hemisphere stratospheric westerlies concentrates planetary scale waves closer to the polar vortex (Watson and Gray 2014). Other explanations of this teleconnection have emphasized the impact of the QBO-MMC on the middle stratosphere (Yamashita et al. 2011; Garfinkel et al. 2012). These studies emphasize that the midlatitude middle stratospheric mean flow geometry is modified by the QBO-MMC in a way that prevents planetary waves, which customarily propagate equatorward through the midlatitude middle stratosphere, from doing so, thereby confining the waves to higher latitudes and weakening the polar vortex (Rao et al. 2021).

One aspect of the Holton–Tan effect is the modulated frequency of sudden stratospheric warmings (SSWs), rapid breakdowns of the stratospheric polar vortex in response to amplification of vertically propagating planetary scale waves. SSWs occur more often during EQBO winters than westerly QBO (WQBO) winters (Labitzke 1982; Anstey et al. 2022) but they can occur during either phase and can initiate persistent hemispheric-scale surface temperature, precipitation, and circulation responses in boreal winter (Butler et al. 2017; Rao et al. 2020c; Noguchi et al. 2020). Given that SSWs have known surface impacts, many of the surface impacts ascribed to the QBO could arise largely from the change in frequency of SSWs during the different QBO phases.

It is also possible that the QBO interacts with the global circulation and the surface "directly," herein defined as in the absence of SSWs. Observational and model-based studies indicate that the QBO has a direct effect on tropical upper-tropospheric–lower-stratospheric conditions (Martin et al. 2021a) and, subsequently, tropical–extratropical planetary wave propagation through the upper troposphere (Yamazaki et al. 2020). Moreover, reanalysis-based studies show that EQBO shifts the tropospheric zonal mean zonal winds in the vicinity of the Northern Hemisphere subtropical jet poleward (White et al. 2015; Hitchman et al. 2021). This has been corroborated in a hierarchy of model simulations (Garfinkel and Hartmann 2011a,b) and even in a simulation in which SSWs are explicitly suppressed (Elsbury et al. 2021a). Model-based evidence also indicates that EQBO is capable of warming the polar stratosphere in a climate model that severely underestimates SSWs (Richter et al. 2008; Garfinkel et al. 2012). These direct effects of the QBO on the atmospheric circulation ostensibly yield surface impacts.

Here, we present results from an ensemble of branched simulations in which EQBO is prescribed in simulations previously devoid of a QBO. These simulations, which run with fixed repeating annual cycles of sea surface temperatures and sea ice, reproduce many of the observed EQBO teleconnections and surface impacts. The ensemble members are then binned based on whether or not an EQBO branched run has a SSW or not and the teleconnections and their associated surface impacts are reevaluated.

2. Methods

The Whole Atmosphere Community Climate Model (WACCM) is used. The model was run with version 4 of the Community Atmosphere Model physics (Neale et al. 2013), which included from WACCM3 an updated parameterization of nonorographic and orographic gravity waves that made the frequency of SSWs more similar to reanalysis (Richter et al. 2010; Marsh et al. 2013). To lower the computational cost of these experiments, the model was run with specified chemistry (SC) in which monthly mean ozone and chemical and shortwave heating rates are prescribed (Smith et al. 2014). Using specified chemistry as opposed to interactive chemistry reduces the frequency of SSWs from 5 to 4 events decade^{-1} (Smith et al. 2014). The atmospheric model includes 66 vertical levels with a model lid at 5.1×10^{-6} hPa and a horizontal resolution of 1.9 latitude × 2.5 longitude. Fixed repeating annual cycles of sea surface temperature and sea ice concentration representative of time averaged 1979–2008 conditions [from the Hadley Centre Sea Ice and Sea Surface Temperature dataset (HadISST), Rayner et al. 2003] are prescribed, and the greenhouse gases were fixed to year 2000 values.

The model was run continuously for 100 years without prescribing a QBO. Since the model does not spontaneously generate a QBO, the tropical stratospheric winds default to weak tropical stratospheric easterlies. This experiment is referred to as the control, and it provides the hundred 1 November restarts that are used to initialize the EQBO branching experiments. In

the branching runs, a downward propagating EQBO is prescribed by continuously relaxing the tropical zonal-mean zonal winds between 86 and 4 hPa toward an idealized EQBO profile using a time constant of 10 days. Details on this QBO profile are in Matthes et al. (2010), and its zonal wind data are from two 28-month sequences of rocketsondes observations (Gray et al. 2001). The target EQBO profiles have easterlies at 50 hPa and westerlies at 10 hPa. The relaxation time scale τ evolves as a function of latitude according to $\tau(\phi) = 1/[\tau_{eq}\exp^{(1/2)(\phi/10^{\circ})}]$, where ϕ is the latitude and τ_{eq} refers to latitudes 2°S–2°N where the nudging is full strength. The model atmosphere freely evolves poleward of 22°S–22°N, while the nudging is half strength one level above and below the nudging domain (4–86 hPa) and zero at all other vertical levels. The 100 EQBO branched runs are each run from 1 November through 31 January. By comparing the 100 EQBO branched runs with the 100 November–January (NDJ) periods from the control, the transient atmospheric response to EQBO is isolated.

In addition to analyzing the bulk (all 100 members, irrespective of intraseasonal polar vortex variability) atmospheric response to EQBO, this study aims to better understand how the occurrence of SSWs during EQBO influences its teleconnections and surface impacts. Central dates of major SSWs are defined as the first day the zonal-mean zonal wind at 10 hPa and 60°N is 0 m s^{-1} or less (Charlton and Polvani 2007). The 100-yr control run includes 29 NDJ winters with SSWs with 2.5th/97.5th percentile confidence intervals of 20–38, obtained by resampling the 100 winters with replacement into groups of 100, documenting the number of winters with SSWs, and repeating this 10 000 times. EQBO branching promotes a statistically significant increase in SSW frequency as 47 winters have SSWs, of which 14 occur the same year as in the control. EQBO "fails" to generate SSWs during 15 of 29 winters that the control does but "induces" SSWs in 33 of 71 winters that the control does not, illustrating that SSWs alone are a strong source of internal variability. The number of winters with SSWs is emphasized in this study as opposed to the number of SSW events. However, if the additional criterion that SSW central dates be separated by 20 consecutive days of westerlies is applied, the control run includes one winter with two SSWs and the EQBO branched runs include four winters with two SSWs bringing the SSW totals to 30 and 51, respectively.

To regulate the influence from SSWs in the control and EQBO ensembles, we discard the 29 control run/EQBO branched run pairs in which the control NDJ winter includes a SSW. This means that of the remaining 71 control run/EQBO branched run pairs, SSWs only occur in the EQBO branched ensemble. The 71 control run/EQBO branched run pairs are then separated into two groups, "EQBO with SSWs," the 33 pairs in which the EQBO branched run includes a SSW, and "EQBO without SSWs," the 38 remaining pairs, which are entirely devoid of SSWs. Partitioning the experiments into these groups and differencing between their respective EQBO branched and control runs isolates, for EQBO with SSWs, the effect of EQBO on the atmospheric circulation when a SSW also occurs. In the case of EQBO without SSWs, we isolate the effect of EQBO on the atmosphere when all types of intraseasonal polar vortex variability are present except for SSWs. This includes more minor perturbations to the polar vortex that may weaken the vortex but do not fully reverse the westerly winds to qualify as a SSW.

3. Results

The control NDJ monthly averaged zonal-mean zonal wind climatologies and standard deviations are shown in the first column of Fig. 1. With no QBO in the control, easterlies are omnipresent in the tropical middle-to-upper stratosphere where there is (unrealistically) little zonal-mean zonal wind variability (Figs. 1a–c). Variability in the winds generally is largest at high latitudes and increases with height. If the control zonal-mean zonal winds are compared against those from ERA5 reanalysis (Hersbach et al. 2020) sampled for 1979 through 2008 (Fig. S1 in the online supplemental material), so as to be consistent with the time-averaged SSTs prescribed in the experiments, it is apparent that the control experiment polar vortex is weaker than observed. This may be due to a number of factors, for instance, the model's polar vortex zonal wind variability, which maximizes too far north (~75°N) compared to observations (~65°N), biases in the model's stationary wave, or perhaps the absence of a QBO. In contrast to these polar stratospheric biases, the strength of the zonally averaged tropospheric jet stream and its variability are better represented by the model.

The 100-member ensemble-mean zonal-mean zonal wind responses in the branched prescribed EQBO experiments are shown in the second column of Fig. 1. During November, the first month after the EQBO nudging is turned on, the tropical lower stratospheric easterlies and middle stratospheric westerlies comprising EQBO are not yet at full strength and so have little effect on the extratropical circulation (Fig. 1d). The QBO westerlies and easterlies gradually protrude into the extratropical Northern Hemisphere during December (Fig. 1e), but it is only during January that tropospheric responses to EQBO develop (Fig. 1f). Consistent with the model, the observed tropical and polar routes are active during December–January or midwinter (Inoue et al. 2011; García-Franco et al. 2022). However, previous observational studies report no statistically significant midwinter subtropical route to the QBO, contrary to what the model shows (Fig. 1f) (Anstey et al. 2010; Gray et al. 2018). Maps of the zonal wind at 200, 500, and 1000 hPa are used to help clarify where the model subtropical route is deriving its signal from (Figs. S2–S4). The 20°–30°N tropospheric easterlies shown in Fig. 1f form in the upper troposphere over western, southern, and eastern Asia as do the anomalous westerlies poleward of these regions. This regional manifestation of the subtropical route is contiguous in height between the upper troposphere and the surface, which it warms.

The EQBO nudging generates a QBO-MMC, which descends and warms the tropics beneath the QBO westerlies, moves poleward, ascends, and cools the midlatitude stratosphere (Fig. 2). The portion of the QBO-MMC beneath the QBO westerlies rotates counterclockwise, while the portion of the QBO-MMC that is more closely associated with the QBO easterlies rotates clockwise. These rotating cells produce midlatitude stratospheric temperature responses that are

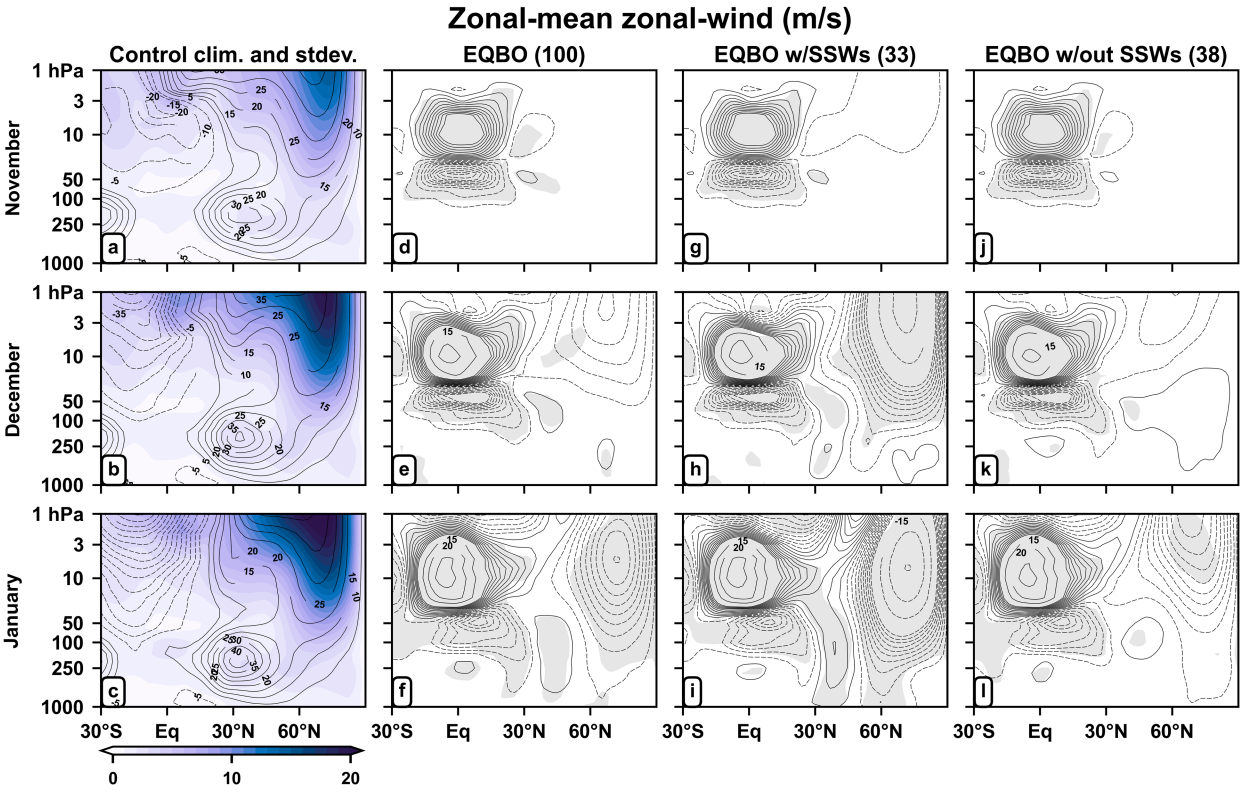

FIG. 1. (a)–(c) Zonal-mean zonal wind control climatologies (contours; ±5 m s^{-1}) and standard deviations (shading). (d)–(l) Responses to prescribing EQBO are shown with contours having intervals of ±25, 20, 15, 9.5, 8.5, 7.5, 6.5, 5.5, 4.5, 3.5, 2.5, 1.5, and 0.5 m s^{-1}. Each row corresponds to a month after branching: (top) November, (middle) December, and (bottom) January. (d)–(f) The 100-member ensemble mean responses to prescribing EQBO. (g)–(i) The response to EQBO events with SSWs, calculated by comparing the 33 EQBO branched runs with SSWs to the 33 control periods from which they were branched. (j)–(l) As in (g)–(i), but for the 38 control run/EQBO branched run pairs in which the EQBO branched runs include no SSW. As stated in the methods section, the 71 control runs considered in (g)–(l) include no SSWs. Gray shading denotes statistical significance, p values < 0.05 retrieved using the two-sample and two-sided bootstrap hypothesis test of Efron and Tibshirani (1994, algorithm 16.2).

opposite in sign with those in the tropics at the same altitudes (Fig. 2d). Over time, the midlatitude stratospheric temperature responses protrude farther into the extratropical Northern Hemisphere (Figs. 2d–f), as do the QBO westerlies and QBO easterlies (Figs. 1d–f). This indicates that the QBO-MMC gradually extends poleward (e.g., Lu et al. 2014; White et al. 2016), which likely results from a combination of the model QBO continuously strengthening (QBO-MMC strength is proportional to the QBO strength, Garfinkel and Hartmann 2011a) and Rossby waves modifying the QBO-MMC's latitudinal extent (White et al. 2016; Haynes et al. 2021).

EQBO forcing persistently weakens and warms the polar vortex one month after the QBO nudging begins, with statistically significant differences in polar vortex strength between the EQBO and control ensembles in January (Figs. 1f and 2f). This can be attributed, although not entirely, to the statistically significant increase in the frequency of winters with SSWs. The central dates of SSWs within the EQBO with SSWs ensemble begin as early as 22 November and end as late as 31 January. All central dates are scattered between these two dates, and no attempt is made to further subsample this already small ensemble. Two of the SSWs in the EQBO with SSW subsample occur during November, 18 during December, and 13 during January. This means, for example, that in our EQBO with SSW response, we are averaging across members with different timings in when the SSW actually occurs, which could be regarded as a limitation. However, in practice, the different timings of the SSWs in each branched run of the EQBO with SSW subsample may not make a substantial difference on our ability to isolate the EQBO and SSW responses. For example, the polar stratospheric zonal-mean zonal wind and temperature responses to EQBO exhibit pronounced differences between the cases (Figs. 1h,k and 2h,k). This is also apparent in Fig. 3, which shows that 10-hPa zonal-mean zonal wind at 60°N is distinctly different when there are SSWs versus when there are not (Figs. 3b,c).

EQBO forcing steadily weakens the ensemble mean polar vortex beginning in December and through January (Fig. 3a). The timing of this polar vortex response is heavily impacted by the EQBO with SSW subsample (Fig. 3b), which features a large attenuation of the polar vortex beginning in December, concurrent with when a statistically significant amplification of wave-1 occurs (Fig. 3e). This wave-1 response is mostly absent without

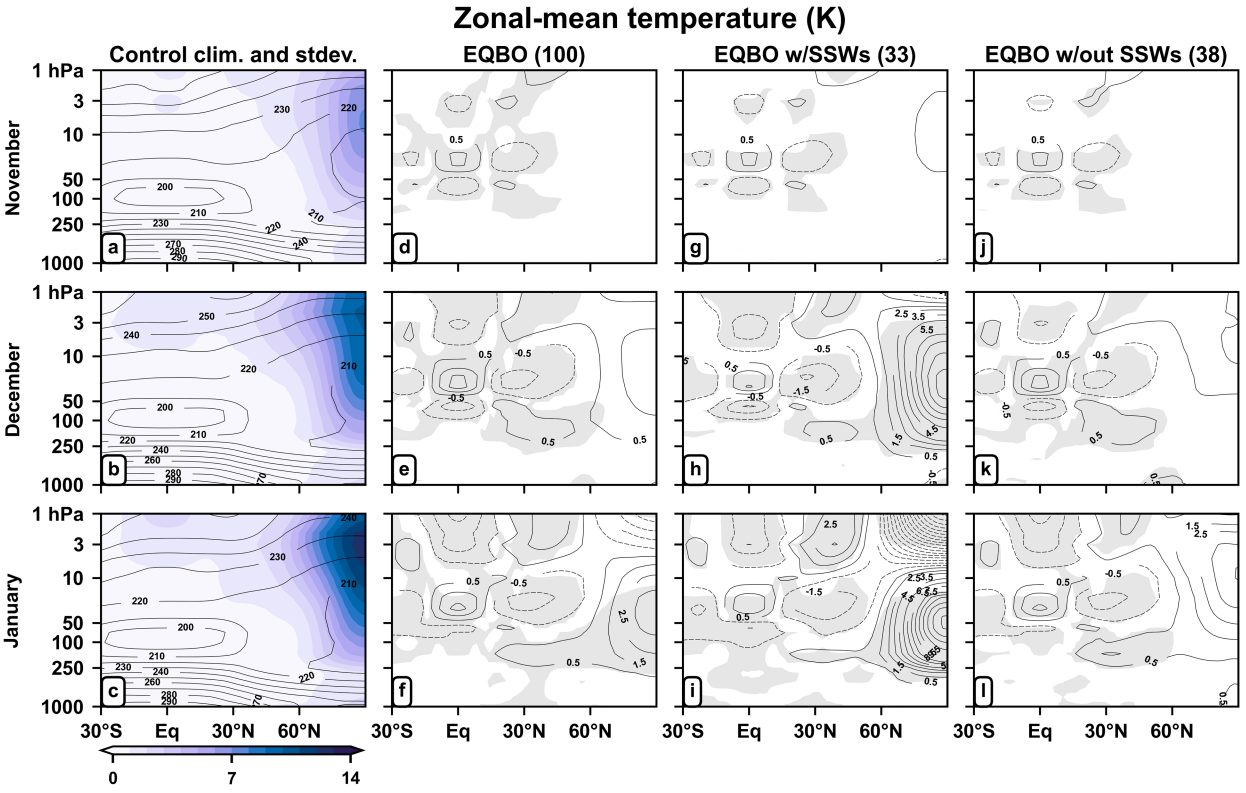

FIG. 2. As in Fig. 1, but showing the zonal mean temperature. The contour intervals for all anomaly plots are ±1 K.

SSWs (Fig. 3f). Thus, even though the SSWs occur at different times, December can be regarded as the primary SSW "forcing month" in these simulations when upward planetary wave propagation through the stratosphere is large (Fig. 3e), and January can be regarded as the primary "impact month" of the SSWs on the tropospheric circulation and surface (due to most SSWs occurring in December and January and their 1–6-week downward propagation time scales). Note that this statistically significant amplification of wave-1 takes place at 50 hPa as well but not at 500 hPa (neither shown), hinting that the source region for the upward component of wave-1 is near the tropopause or above. To understand this further, we do a Fourier analysis of the geopotential height response to EQBO and filter for zonal wavenumber one (wave-1) at 100 hPa (Fig. S5) and 500 hPa (Fig. S6). The anomalous wave-1 response present in EQBO with SSWs is largely barotropic between 50 hPa (not shown) and 500 hPa (Fig. S6), but only in the stratosphere, do the anomalous wave-1 geopotential heights constructively interfere (e.g., Fletcher and Kushner 2011) during December with the climatological wave-1 heights. Hence, the enhancement of wave-1 in EQBO with SSWs is taking place near and above the tropopause in this model.

Interestingly, EQBO still promotes statistically significant weakening of the upper polar stratospheric winds during January in the absence of SSWs (Fig. 1l). This coincides with 4–5 K of nonstatistically significant polar stratospheric warming during January (Fig. 2l) and Fig. 3c further highlights that EQBO persistently weakens the polar vortex without SSWs beginning in mid-December, though this response is only somewhat statistically significant. These results indicate that the polar vortex still weakens and warms in the absence of SSWs given EQBO, just slower relative to the warming brought on by the SSWs. Note, however, that this result may partially arise from not considering the 29 EQBO branched run/control run pairs in which the control has an SSW, such that the control background state against which the 38 no-SSW EQBO perturbation runs are compared is artificially cool, which helps to reveal the polar stratospheric warming. If all 100 control run/EQBO branched run pairs are considered instead, there is no statistically significant weakening of the polar vortex in the EQBO without SSWs ensemble; however, the EQBO with SSW responses are largely unchanged (Fig. S7).

Using the EQBO with SSWs and the EQBO without SSWs ensembles, we can assess if or how EQBO influences the subtropical and polar routes of surface influence in the presence and absence of SSWs. However, the sensitivity of EQBO's tropical route to SSWs, via changes in the Brewer–Dobson circulation, for example (e.g., Noguchi et al. 2020; Hood et al. 2023), cannot be assessed because EQBO is prescribed (so the SSWs cannot modulate the circulation in the tropical nudged region). EQBO forcing accelerates the tropical upper-tropospheric winds via the tropical route in both the EQBO with SSWs and EQBO without SSW subsamples (Fig. 1).

The subtropical route, represented by a poleward shift of the subtropical jet (Fig. 1f), at first glance appears to be modulated in magnitude and extension to the surface by the presence of SSWs (Figs. 1i,l). EQBO with SSWs exhibits an

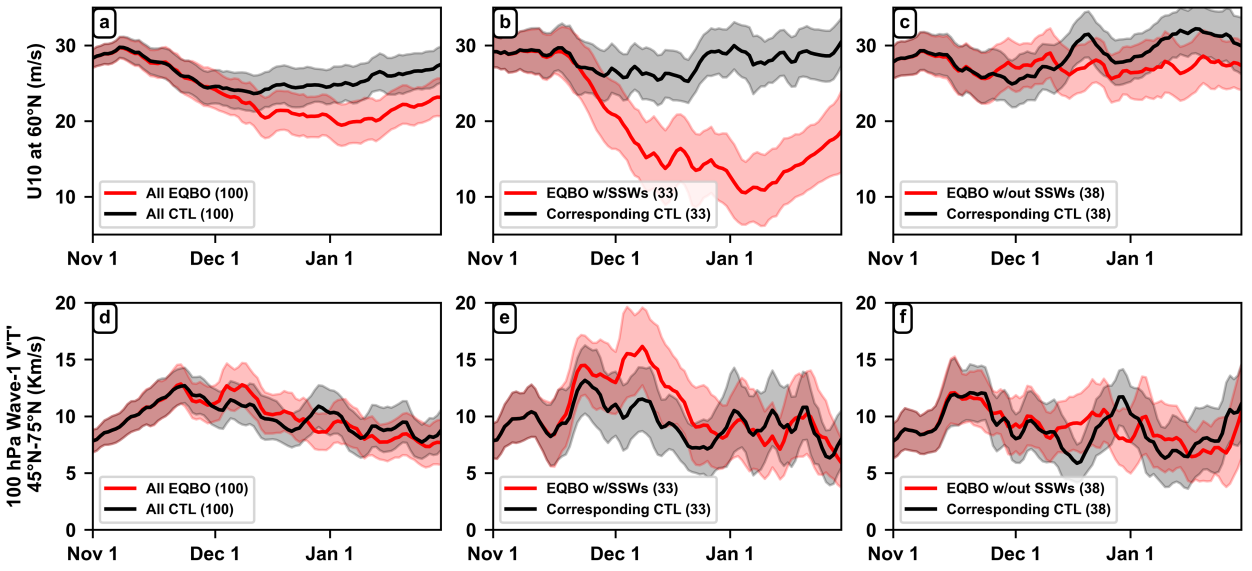

FIG. 3. The 10-hPa zonal mean zonal wind at 60°N in the EQBO branched runs and control shown as a function of time. (a) The 100-member ensemble mean responses. The EQBO (b) with SSW responses and (c) without SSW responses. The bootstrapped 2.5th/97.5th percentile confidence intervals are shown around each solid curve. (d)–(f) As in (a)–(c), but for the 100-hPa wave-1 eddy heat flux latitudinally averaged (with cosine weighting) between 45° and 75°N.

intensified and poleward shifted subtropical jet as early as December, with the jet strengthening on the poleward flank of the subtropical jet surpassing 2.5 m s^{-1} by January (Fig. 1i). On the other hand, this response and in particular its extension to the subtropical surface is not seen in EQBO without SSWs. While Fig. 1 gives the impression that the subtropical route only develops in winters with SSWs, this is partly an artifact of averaging the zonal wind over all longitudes. Both the North Atlantic and Pacific sector tropospheric zonal winds differ between the EQBO with SSW and EQBO without SSW subsamples (e.g., Fig. 6). Yet over Asia, subtropical route zonal wind anomalies descend into the troposphere irrespective of SSWs (Figs. S2–S4), which is not evident from Fig. 1. Hence, the apparent differences in the zonal-mean subtropical route with and without SSWs result from different regional circulation processes projecting onto the zonal-mean wind, including differences in wave driving between the two ensembles (e.g., reinforced Aleutian low), different downward effects of polar vortex variability projecting onto the subtropical route (e.g., the negative NAO response), and the regional manifestation of the subtropical route over Asia.

The sensitivity of the EQBO subtropical and polar routes to SSWs suggests that the surface impacts may also vary depending on whether or not SSWs occur. A negative NAO-like surface response develops in the ensemble mean (all 100 members) response during January, along with cooling over Eurasia and warming over Greenland, northern Africa, and the Middle East (Fig. 4f). These NAO-associated surface impacts of the QBO have been reported frequently in the literature (Angell et al. 1969; Holton and Tan 1980; Anstey and Shepherd 2014; Gray et al. 2018; Zhang et al. 2019; Andrews et al. 2019; O'Reilly et al. 2019; Rao et al. 2020b; Zuo et al. 2022). After subsampling for SSWs versus non-SSWs, it is found that the increased frequency of SSWs during EQBO is primarily responsible for the negative NAO-like surface circulation and temperature responses, including the Baffin Bay/Greenland warming, most of the northern Africa warming, and some of the Eurasian cooling (cf. Figs. 4f,i,l). Regarding the latter, EQBO forcing generates Eurasian cooling in the absence of SSWs as well (Fig. 4l). The +3-hPa surface ridge over the Arctic and Eurasia that may be responsible for this cooling is not statistically significant, but the EQBO is still weakening the polar vortex without SSWs (Fig. 1l), which could mean there is mass accumulating in the polar stratosphere that is exerting more pressure on the surface. This may mean that this is merely a side effect of not being able to completely remove periods when the polar vortex is weak, even though no major SSWs occur in the EQBO without SSW subsample.

Across all 100 members, surface temperatures increase over central Asia once EQBO is prescribed, corroborating observational studies (reanalysis and station-based temperature measurements) that have reported that the sign of the QBO's lower stratospheric winds is anticorrelated with surface temperatures there (Chen and Li 2007; Ma et al. 2021; Park et al. 2022; Zuo et al. 2022). The warming is present on the southeastern side of an anomalous surface trough that develops over Asia during December and January (Figs. 4e,f). This trough destructively interferes with the climatological ridge over the continent, the Siberian High, which ordinarily prompts northerly flow on its eastern side. The warming and its collocated trough migrate equatorward and slightly eastward in January, as do the 200-hPa zonal wind (Fig. S2) and 200-hPa velocity potential (not shown) responses over Asia. The surface warming over Asia is apparent with or without SSWs (Figs. 4g–l), implying that this is a "direct" response to EQBO. The collocation between the zonal wind anomalies over Asia (Figs. S2–S4) and the surface warming affirms that the subtropical route promotes this surface impact. Note that the anomalous surface trough over Asia during

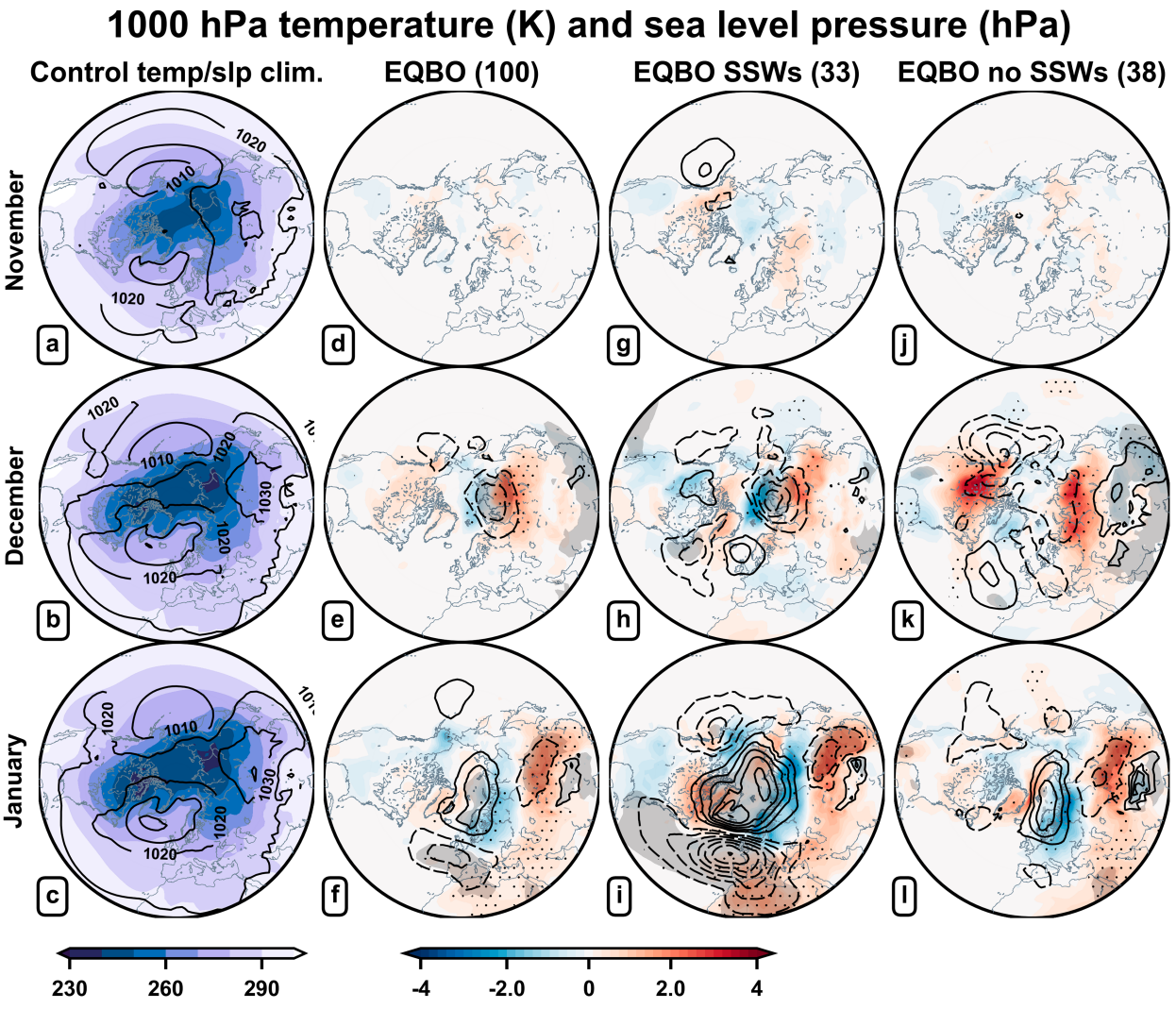

FIG. 4. (a)–(c) The 1000-hPa temperature (shading) and sea level pressure (contours; 10-hPa intervals) control experiment climatologies. (d)–(l) Temperature responses to prescribing EQBO are shown with red and blue shading, and sea level pressure responses are shown in black contours (±1 hPa). (d)–(f) The 100-member ensemble mean responses to prescribing EQBO. (g)–(i) The EQBO with SSW responses and (j)–(l) the EQBO without SSW responses. Stippling (gray undershading) denotes statistical significance.

December (Fig. 4e) is stronger in the case with SSWs (Fig. 4h) and weaker in the case without SSWs (Fig. 4k). This difference in the strength of the trough appears to be related to opposite phase synoptic-scale wave trains propagating over the Atlantic and Eurasia depending on if there are SSWs or not (Figs. 4h,k); these wave trains bear some resemblance to the Scandinavian pattern (Pang et al. 2022). Surface pressures are higher over Southeast Asia in the absence of SSWs during December, reinforcing the warming over the continent, while promoting some cooling over the South China Sea (Fig. 4k).

For the most part, the surface temperature response to EQBO is weak over North America. However, expansive surface warming occurs over the northern part of the continent in the absence of SSWs during December (Fig. 4k). This warming may develop in association with the nonstatistically significant Alaska surface trough. It is worth mentioning that some of these nonsignificant features may arise due to sampling variability.

Imposing EQBO has global effects on precipitation. Broadly speaking, the ensemble-mean response to EQBO features reduced precipitation over the Indian Ocean and increased precipitation over the tropical western Pacific and over some of the Maritime Continent, with the strongest regional response being a +50-mm increase between Indonesia and western Australia during January (Figs. 5e,f). Coinciding with the reduced Indian Ocean precipitation, longitude–pressure cross sections of the tropical (10°S–10°N) velocity potential response reveal that convergence is taking place in the upper troposphere over the Indian Ocean while divergence increases directly below in the lower troposphere, both of which indicate that anomalous descent takes place over the Indian Ocean in response to the EQBO perturbation (not shown). Similar observational responses appear in

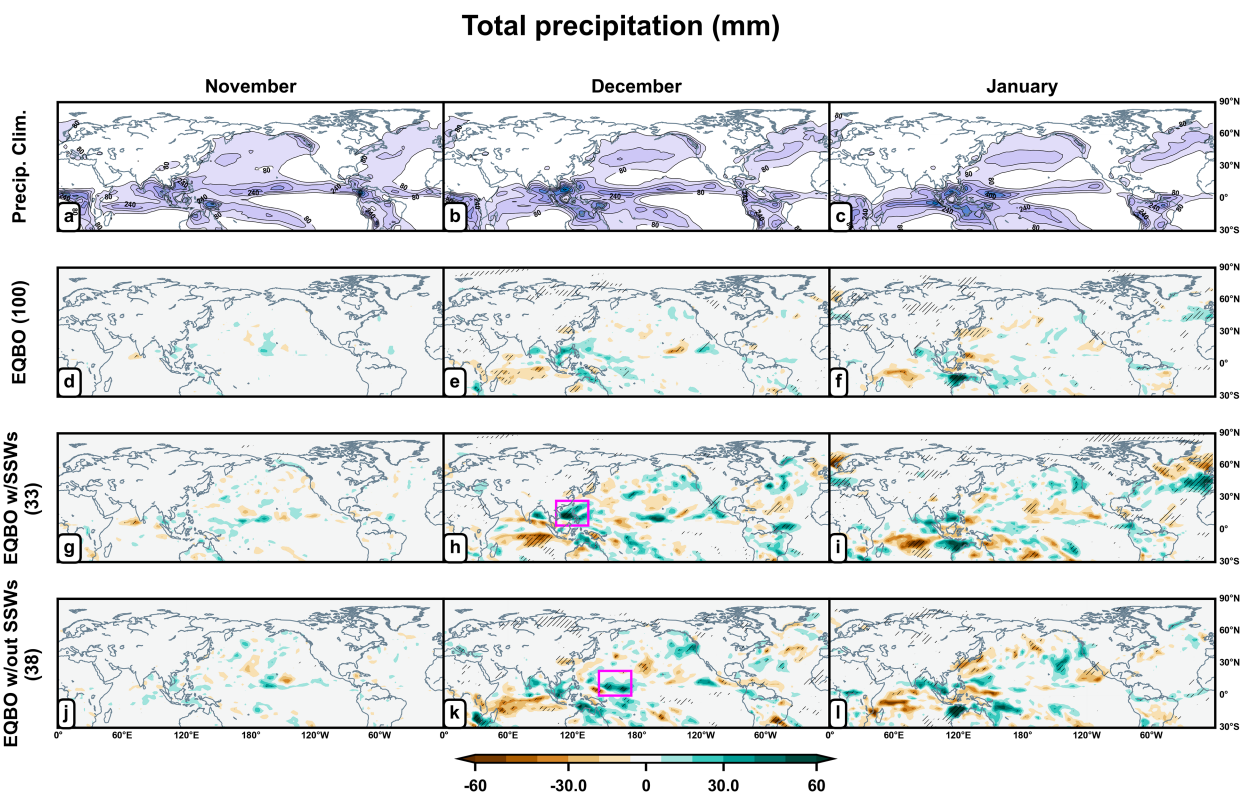

FIG. 5. (a)–(c) Climatological monthly precipitation totals for November through January. (d)–(f) Precipitation responses to prescribing EQBO are shown in green and brown shading. (g)–(i) As in (d)–(f), but for the EQBO with SSW subsample. (j)–(l) As in (d)–(f), but for the EQBO without SSW subsample. The magenta box in (h) is located between 4°–27°N and 105°–135°E. The magenta box in (k) is located between 0°–23°N and 145°–175°E. Hatching denotes statistical significance.

Yamazaki et al. (2020) and in Rao et al. (2020a), who showed that CMIP6 models miss these signals. In the extratropics, regional responses develop over the North Atlantic and Europe during January, where precipitation shifts south consistent with a negative NAO response to EQBO (Fig. 5f).

Large differences in precipitation between SSW and non-SSW cases are found over the North Atlantic and Europe. In the EQBO case with SSWs, during January, the SSWs shift the storm track and precipitation south over the North Atlantic and Europe (e.g., Butler et al. 2017; Ayarzagüena et al. 2018), which is entirely absent without SSWs (Figs. 5i,l). This indicates that the increased frequency of SSWs during EQBO is primarily responsible for the ensemble mean (all 100 members) southward shift of precipitation over the North Atlantic and Europe (cf. Figs. 5f,i). There are also differences in precipitation with and without SSWs over the South China Sea. With SSWs, precipitation increases over the South China Sea during December (box, Fig. 5h); recall that December is the SSW forcing month in which stratospheric wave-1 driving is strong. This regional precipitation response is mostly absent without SSWs when instead the increases in precipitation are relatively strong just west of the international date line (box, Fig. 5k). Noting that tropical–subtropical precipitation influences tropical–extratropical planetary wave propagation (Scaife et al. 2017), these longitudinal differences in where the precipitation occurs hint that tropical–extratropical planetary wave propagation varies in the SSW versus no SSW cases.

Figures 6a–c show the climatological stationary wave field, which is retrieved by removing the long-term (100-yr average) daily zonal-mean geopotential height from the full daily geopotential height field. While there are some differences in amplitude relative to reanalysis (not shown), the model reproduces the climatological stationary wave at 200 hPa, including the East Asia trough, the Alaskan Ridge, the Baffin Bay trough, and the North Atlantic ridge (Figs. 6a–c).

The ensemble mean response to EQBO features a statistically significant increase in geopotential height over Asia during January, that is present irrespective of SSWs, providing further evidence that EQBO has a direct effect on the circulation over these longitudes (Figs. 6f,i,l). This anticyclonic anomaly is also apparent in the U200 response (Fig. S2). In the zonal mean, the Asia anticyclone and the North Pacific anticyclone (see Rao et al. 2020a) show up as a poleward shifted subtropical jet (cf. Fig. 1f). The anticyclone is the signature of the subtropical route and is contiguous through the troposphere to the surface.

The geopotential height fields during EQBO vary depending on when there are SSWs versus when there are not. In the case with SSWs, a nonstatistically significant tropical–extratropical wave train is visible in December just poleward of the South

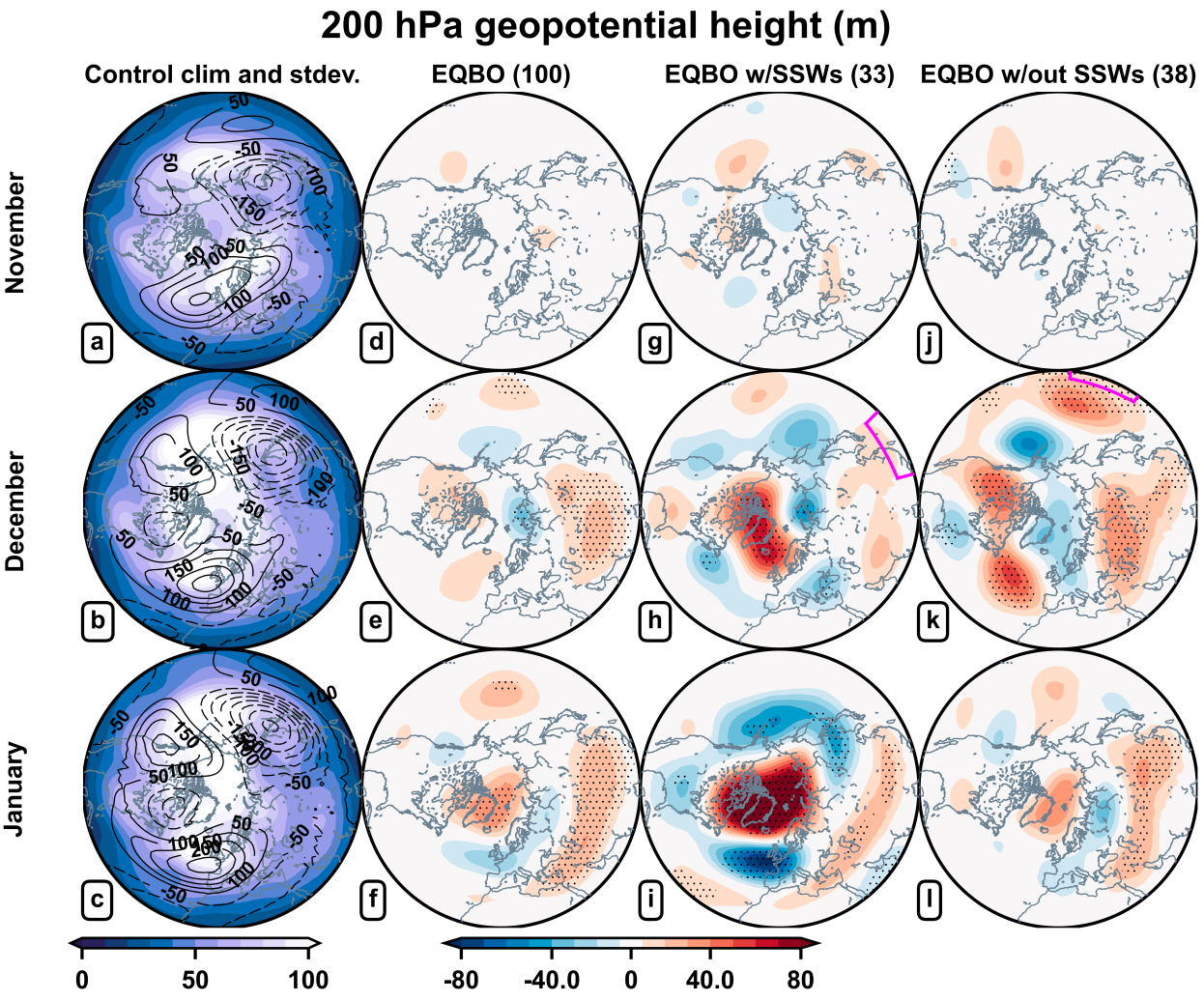

FIG. 6. As in Fig. 1, but showing (a)–(c) 200-hPa eddy height field climatologies (contours; ±50 m) and climatological standard deviations (shading) and (d)–(l) full 200-hPa geopotential height anomalies. The magenta boxes in Figs. 5e and 5h are overlaid on (h) and (k) to highlight the collocation between the precipitation and wavetrain responses. Stippling denotes statistical significance.

China Sea where the increase in precipitation was previously observed (magenta line, cf. Figs. 5e and 6h). The extratropical trough of this wave train constructively interferes with the climatological wave-1 scale East Asia trough (cf. Figs. 6b,h), which is likely a part of the forcing giving rise to the increased 100-hPa eddy heat flux shown in December in Fig. 3e. Conversely, a synoptic-scale tropical–extratropical wave propagates over the North Pacific during December in the absence of SSWs, also interfering constructively with parts of the stationary wave (Fig. 6k). Of note, this synoptic wave train emanates from the subtropics just west of the international date line, the same region where the precipitation maxima was observed in the absence of SSWs (magenta line, cf. Figs. 5h and 6k). These results hint that the difference between having a SSW and not in the EQBO runs is partly dependent on the state of the tropics (i.e., where convective heating is occurring, which can change the location of extratropical wave propagation and whether the wave constructively or destructively interferes with the climatological stationary wave). Note too, there are opposite signed wave trains over the North Atlantic during December in the SSW versus no SSW cases whose signature is also apparent in the sea level pressure responses of Fig. 4.

4. Discussion and conclusions

There are limitations to our modeling and analysis approach that could influence how applicable this idealized study is to the real world. First, the model results would probably be more realistic if EQBO was prescribed earlier than 1 November. The observed extratropical stratospheric vorticity response to EQBO is underway during October and November (White et al. 2016; Lu et al. 2020; Silverman et al. 2021), which is before there is any extratropical stratospheric response to prescribed EQBO in these runs (Fig. 1). Second, the model simulations use specified chemistry, which neglects interactions between planetary waves and ozone anomalies, affecting planetary wave–mean

flow interactions (Silverman et al. 2018), thereby muddying their effect on the secondary circulation (e.g., Lin and Ming 2021). Third, our analysis approach attempts to isolate the direct influence of the EQBO polar route on the surface by removing major SSWs; however, we are not able to fully remove all internal polar vortex variability using this method, and minor warmings or other types of vortex variability may still be influencing the results. Nonetheless, Fig. 3 suggests that the composite approach reasonably separates winters with strong vortex perturbations from those without. Additionally, we find no difference in downward wave coupling (DWC) event frequency between the control and the EQBO branched ensembles (Table S1), so that it is unlikely we are inadvertently compositing across a different type of polar vortex event in any systematic way.

Despite the limitations of the modeling and analysis approach, these results raise questions about how both the subtropical and polar routes of the QBO impact the surface. In particular, is the increased occurrence of SSWs necessary for there to be surface impacts during EQBO? Or is there a direct effect of the EQBO even in the absence of SSWs? As other studies have shown and these results corroborate, SSWs occur more often during EQBO. We show that this increased frequency of SSWs is responsible for most (though not all) of the surface impacts over the North Atlantic, southern Europe, and North Africa. This is important because it implies that attempts at leveraging the QBO for Subseasonal to Seasonal Prediction project (S2S) of NAO variability may be impacted by the ability to predict SSWs, which are currently skillfully predicted by operational forecast systems out to nearly two weeks (Domeisen et al. 2020; Lawrence et al. 2023).

The subtropical route is found to descend into the troposphere over western, central, and eastern Asia in response to EQBO irrespective of SSWs and promote surface warming over these regions. ERA5 yields similar results, which exhibit some sensitivity to ENSO (Figs. S8 and S9). These results are, to the best of our knowledge, the first GCM simulations showing warmer temperatures over Asia once EQBO conditions are imposed, corroborating Chen and Li (2007) and Zuo et al. (2022) who used reanalysis and station surface temperature observations over China, and Ma et al. (2021) who also attributed the surface warming to the subtropical route. This regional jet response is masked by zonal averaging (e.g., Fig. 1) and is more readily visible in zonal wind maps (Figs. S2–S4). More research is needed to better understand this teleconnection, especially since precedent shows the subtropical route to form in jet exit regions mainly during late winter (Garfinkel and Hartmann 2011a; Gray et al. 2018). Inoue and Takahashi (2013) also detected subtropical route zonal wind anomalies over this region in reanalysis plus adiabatic descent throughout the troposphere, both of which were attributed to the regional wave–mean flow interactions.

The enhancement in SSW frequency is coincident with the amplification of wave-1, which is absent for winters without SSWs. Studies have reported for decades that EQBO amplifies stratospheric wave-1 (Holton and Tan 1980; Labitzke 1982; Garfinkel et al. 2012; Watson and Gray 2014; Lu et al. 2020; Ma et al. 2021; Silverman et al. 2021). An open question is whether this amplification in wave-1 driving is forced by the EQBO itself or just arises stochastically (and then interacts with the mean flow modulated by the EQBO to preferentially drive SSWs). Yamazaki et al. (2020) showed that the tropical tropospheric response to EQBO, when imposed in a simplified model, stimulates horizontal planetary wave propagation out of the tropical upper troposphere into the extratropics in a manner that could reinforce upward planetary wave propagation via the climatological East Asia trough. This mechanism may explain why Elsbury et al. (2021a) found enhanced December–January upward Plumb (1985) $k = 1$–3 wave activity flux over the North Pacific and East Asia at 50 hPa during EQBO using the same model that we use here. That same study also found the just mentioned upward wave activity flux response to EQBO in a separate sensitivity simulation with fixed repeating annual cycles of present-day SST/SIC, a prescribed QBO, and suppressed (by nudging toward climatology) polar stratospheric variability (<200 hPa, poleward of 60°N). These findings indicate that EQBO enhances upward planetary wave propagation over the North Pacific somewhat independently of internally generated polar stratospheric variability. However, we only find the enhancement of wave-1 due to EQBO when SSWs occur, indicating that internal variability projects onto EQBO's pathway to influence wave-1. One hypothesis is that the different tropical–subtropical western Pacific precipitation responses to EQBO with and without SSWs influence the trajectory of the Rossby waves propagating into the extratropics (cf. Figs. 5h,k with Figs. 6h,k) and therefore whether or not the climatological stationary wave is reinforced (see Scaife et al. 2017).

In contrast to the known influence of EQBO on increasing SSW frequency, EQBO warms the polar stratosphere even in the absence of SSWs, which suggests a role for a direct stratospheric pathway for the QBO to influence the polar vortex. This parallels Garfinkel et al. (2012) who found that prescribing EQBO in an ensemble of 1 January branched runs promoted polar stratospheric warming despite few SSWs. Polar stratospheric warming in response to EQBO has been explained as an effect of the middle stratospheric mean flow response to the QBO-MMC (Yamashita et al. 2011; Garfinkel et al. 2012; Lu et al. 2014; Rao et al. 2021). Rao et al. (2021) showed that strength and speed with which the polar stratosphere responds to prescribed EQBO varies depending on when in the annual cycle the nudging is applied. In their study, the polar stratospheric response to EQBO given perpetual early winter radiative forcing developed more slowly than the response given perpetual mid- and late-winter radiative forcing. Seeing as our branched runs begin 1 November, their results may explain why the polar stratospheric warming is relatively slow to develop in EQBO without SSWs. The fact that the polar stratospheric warming takes until January to form (Fig. 2l) is important because there are indications that this pathway has a direct surface impact at high latitudes, enhancing surface pressure at the polar surface, thereby warming Greenland and cooling Europe (Fig. 4l). If this direct polar pathway develops more rapidly during middle and late winter than during early winter (e.g., Rao et al. 2021), perhaps our 3-month branched simulations are complete before the suspected high-latitude response mediated through this pathway is fully formed, which is

motivation to use longer branched simulations (e.g., branch in August, run through April).

The persistence and predictability of the QBO as well as its connection to surface impacts in observations and in idealized studies substantiates the importance of continued efforts to leverage the QBO for S2S predictability. However, the QBO is not internally generated in the majority of S2S forecast models, and in most cases, the QBO winds begin to decay within 2 weeks after initialization (Lawrence et al. 2022). The lack of sustained QBO wind forcing subsequently degrades the QBO's extratropical teleconnections. Though the polar route can be simulated by some S2S forecast systems (Garfinkel et al. 2018; Domeisen et al. 2020; Portal et al. 2022), often the teleconnection is too weak or its timing is inconsistent with observations, both of which may preclude QBO-related surface impacts (e.g., Butler et al. 2016). Poor simulation of the QBO in models may also affect modes of tropical convection; in particular, the observed connection between the QBO and the Madden–Julian oscillation (MJO) is not well captured by most S2S forecast systems (Kim et al. 2019; Martin et al. 2021b; Lawrence et al. 2023). Nonetheless, statistical models suggest that QBO modulation of extratropical teleconnections associated with the MJO imparts significant "windows of opportunity" for improved predictive skill of North American atmospheric rivers and climate on S2S time scales (e.g., Baggett et al. 2017; Mundhenk et al. 2018; Nardi et al. 2020), suggesting that improvement of both QBO and MJO processes may improve dynamical forecasts of extratropical weather. In addition, our results and observational studies (Inoue and Takahashi 2013; Ma et al. 2021) imply that further exploration of the QBO subtropical route for S2S prediction over Asia in particular is warranted. Considering QBO interactions with other types of internal variability, which are explicitly ignored in these fixed boundary condition experiments (e.g., El Niño–Southern Oscillation), may be another topic for future S2S research. For example, the polar route and its relationship with the NAO is more statistically robust during La Niña than during El Niño (Wei et al. 2007; Kumar et al. 2022; Ma et al. 2023), which may have implications for when the QBO provides windows of opportunity for enhanced extratropical predictive skill.

Acknowledgments. We appreciate literature recommendations, input, and questions from Chaim Garfinkel, James Anstey, Hua Lu, and Lon Hood prior to submission, which helped improve this manuscript. We also appreciate the high-performance computing support provided by the National Center for Atmospheric Research, sponsored by the National Science Foundation (NSF). https://doi.org/10.5065/D6RX99HX. Dillon Elsbury was supported in part by NOAA Cooperative Agreements NA17OAR4320101 and NA22OAR4320151.

Data availability statement. The model data provided in this study are available at https://csl.noaa.gov/groups/csl8/modeldata/.

REFERENCES

Andrews, M. B., J. R. Knight, A. A. Scaife, Y. Lu, T. Wu, L. J. Gray, and V. Schenzinger, 2019: Observed and simulated teleconnections between the stratospheric Quasi-Biennial Oscillation and Northern Hemisphere winter atmospheric circulation. *J. Geophys. Res. Atmos.*, **124**, 1219–1232, https://doi.org/10.1029/2018JD029368.

Angell, J. K., J. Korshover, and G. F. Cotten, 1969: Quasi-biennial variations in the "centers of action". *Mon. Wea. Rev.*, **97**, 867–872, https://doi.org/10.1175/1520-0493(1969)097<0867:QVITOA>2.3.CO;2.

Anstey, J. A., and T. G. Shepherd, 2014: High-latitude influence of the quasi-biennial oscillation. *Quart. J. Roy. Meteor. Soc.*, **140** (678), 1–21, https://doi.org/10.1002/qj.2132.

——, ——, and J. F. Scinocca, 2010: Influence of the quasi-biennial oscillation on the extratropical winter stratosphere in an atmospheric general circulation model and in reanalysis data. *J. Atmos. Sci.*, **67**, 1402–1419, https://doi.org/10.1175/2009JAS3292.1.

——, and Coauthors, 2022: Teleconnections of the Quasi-Biennial Oscillation in a multi-model ensemble of QBO-resolving models. *Quart. J. Roy. Meteor. Soc.*, **148**, 1568–1592, https://doi.org/10.1002/qj.4048.

Ayarzagüena, B., D. Barriopedro, J. M. Garrido-Perez, M. Abalos, A. de la Cámara, R. García-Herrera, N. Calvo, and C. Ordóñez, 2018: Stratospheric connection to the abrupt end of the 2016/2017 Iberian drought. *Geophys. Res. Lett.*, **45**, 12 639–12 646, https://doi.org/10.1029/2018GL079802.

Baggett, C. F., E. A. Barnes, E. D. Maloney, and B. D. Mundhenk, 2017: Advancing atmospheric river forecasts into subseasonal-to-seasonal time scales. *Geophys. Res. Lett.*, **44**, 7528–7536, https://doi.org/10.1002/2017GL074434.

Butler, A. H., and Coauthors, 2016: The climate-system historical forecast project: Do stratosphere-resolving models make better seasonal climate predictions in boreal winter? *Quart. J. Roy. Meteor. Soc.*, **142**, 1413–1427, https://doi.org/10.1002/qj.2743.

——, J. P. Sjoberg, D. J. Seidel, and K. H. Rosenlof, 2017: A sudden stratospheric warming compendium. *Earth Syst. Sci. Data*, **9**, 63–76, https://doi.org/10.5194/essd-9-63-2017.

Charlton, A. J., and L. M. Polvani, 2007: A new look at stratospheric sudden warmings. Part I: Climatology and modeling benchmarks. *J. Climate*, **20**, 449–469, https://doi.org/10.1175/JCLI3996.1.

Chen, W., and T. Li, 2007: Modulation of Northern Hemisphere wintertime stationary planetary wave activity: East Asian climate relationships by the Quasi-Biennial Oscillation. *J. Geophys. Res.*, **112**, D20120, https://doi.org/10.1029/2007JD008611.

Densmore, C. R., E. R. Sanabia, and B. S. Barrett, 2019: QBO influence on MJO amplitude over the maritime continent: Physical mechanisms and seasonality. *Mon. Wea. Rev.*, **147**, 389–406, https://doi.org/10.1175/MWR-D-18-0158.1.

Domeisen, D. I. V., and Coauthors, 2020: The role of the stratosphere in subseasonal to seasonal prediction: 2. Predictability arising from stratosphere-troposphere coupling. *J. Geophys. Res. Atmos.*, **125**, e2019JD030923, https://doi.org/10.1029/2019JD030923.

Efron, B., and R. J. Tibshirani, 1994: *An Introduction to the Bootstrap*. 1st ed. CRC Press, 456 pp.

Elsbury, D., Y. Peings, and G. Magnusdottir, 2021a: Variation in the Holton–Tan effect by longitude. *Quart. J. Roy. Meteor. Soc.*, **147**, 1767–1787, https://doi.org/10.1002/qj.3993.

——, ——, and ——, 2021b: CMIP6 models underestimate the Holton-Tan effect. *Geophys. Res. Lett.*, **48**, e2021GL094083, https://doi.org/10.1029/2021GL094083.

Fletcher, C. G., and P. J. Kushner, 2011: The role of linear interference in the annular mode response to tropical SST forcing. *J. Climate*, **24**, 778–794, https://doi.org/10.1175/2010JCLI3735.1.

García-Franco, J. L., L. J. Gray, S. Osprey, R. Chadwick, and Z. Martin, 2022: The tropical route of quasi-biennial oscillation (QBO) teleconnections in a climate model. *Wea. Climate Dyn.*, **3**, 825–844, https://doi.org/10.5194/wcd-3-825-2022.

Garfinkel, C. I., and D. L. Hartmann, 2011a: The influence of the quasi-biennial oscillation on the troposphere in winter in a hierarchy of models. Part I: Simplified dry GCMs. *J. Atmos. Sci.*, **68**, 1273–1289, https://doi.org/10.1175/2011JAS3665.1.

——, and ——, 2011b: The influence of the quasi-biennial oscillation on the troposphere in winter in a hierarchy of models. Part II: Perpetual winter WACCM runs. *J. Atmos. Sci.*, **68**, 2026–2041, https://doi.org/10.1175/2011JAS3702.1.

——, T. A. Shaw, D. L. Hartmann, and D. W. Waugh, 2012: Does the Holton–tan mechanism explain how the quasi-biennial oscillation modulates the Arctic polar vortex? *J. Atmos. Sci.*, **69**, 1713–1733, https://doi.org/10.1175/JAS-D-11-0209.1.

——, C. Schwartz, D. I. V. Domeisen, S.-W. Son, A. H. Butler, and I. P. White, 2018: Extratropical atmospheric predictability from the quasi-biennial oscillation in subseasonal forecast models. *J. Geophys. Res. Atmos.*, **123**, 7855–7866, https://doi.org/10.1029/2018JD028724.

Gray, L. J., S. J. Phipps, T. J. Dunkerton, M. P. Baldwin, E. F. Drysdale, and M. R. Allen, 2001: A data study of the influence of the equatorial upper stratosphere on Northern-Hemisphere stratospheric sudden warmings. *Quart. J. Roy. Meteor. Soc.*, **127**, 1985–2003, https://doi.org/10.1002/qj.49712757607.

——, J. A. Anstey, Y. Kawatani, H. Lu, S. Osprey, and V. Schenzinger, 2018: Surface impacts of the Quasi Biennial Oscillation. *Atmos. Chem. Phys.*, **18**, 8227–8247, https://doi.org/10.5194/acp-18-8227-2018.

Hansen, F., K. Matthes, and L. J. Gray, 2013: Sensitivity of stratospheric dynamics and chemistry to QBO nudging width in the chemistry-climate model WACCM. *J. Geophys. Res. Atmos.*, **118**, 10 464–10 474, https://doi.org/10.1002/jgrd.50812.

Haynes, P., P. Hitchcock, M. Hitchman, S. Yoden, H. Hendon, G. Kiladis, K. Kodera, and I. Simpson, 2021: The influence of the stratosphere on the tropical troposphere. *J. Meteor. Soc. Japan*, **99**, 803–845, https://doi.org/10.2151/jmsj.2021-040.

Hersbach, H., and Coauthors, 2020: The ERA5 global reanalysis. *Quart. J. Roy. Meteor. Soc.*, **146**, 1999–2049, https://doi.org/10.1002/qj.3803.

Hitchman, M. H., S. Yoden, P. H. Haynes, V. Kumar, and S. Tegtmeier, 2021: An observational history of the direct influence of the stratospheric quasi-biennial oscillation on the tropical and subtropical upper troposphere and lower stratosphere. *J. Meteor. Soc. Japan*, **99**, 239–267, https://doi.org/10.2151/jmsj.2021-012.

Holton, J. R., and H.-C. Tan, 1980: The influence of the equatorial quasi-biennial oscillation on the global circulation at 50 mb. *J. Atmos. Sci.*, **37**, 2200–2208, https://doi.org/10.1175/1520-0469(1980)037<2200:TIOTEQ>2.0.CO;2.

Hood, L. L., N. E. Trencham, and T. J. Galarneau Jr., 2023: QBO/solar influences on the tropical Madden-Julian oscillation: A mechanism based on extratropical wave forcing in late fall and early winter. *J. Geophys. Res. Atmos.*, **128**, e2022JD037824, https://doi.org/10.1029/2022JD037824.

Inoue, M., and M. Takahashi, 2013: Connections between the stratospheric quasi-biennial oscillation and tropospheric circulation over Asia in northern autumn. *J. Geophys. Res. Atmos.*, **118**, 10 740–10 753, https://doi.org/10.1002/jgrd.50827.

——, M. Takahashi, and H. Naoe, 2011: Relationship between the stratospheric quasi-biennial oscillation and tropospheric circulation in northern autumn. *J. Geophys. Res.*, **116**, D24115, https://doi.org/10.1029/2011JD016040.

Karpechko, A. Y., N. L. Tyrrell, and S. Rast, 2021: Sensitivity of QBO teleconnection to model circulation biases. *Quart. J. Roy. Meteor. Soc.*, **147**, 2147–2159, https://doi.org/10.1002/qj.4014.

Kim, H., J. H. Richter, and Z. Martin, 2019: Insignificant QBO-MJO prediction skill relationship in the SubX and S2S subseasonal reforecasts. *J. Geophys. Res. Atmos.*, **124**, 12 655–12 666, https://doi.org/10.1029/2019JD031416.

Kumar, V., S. Yoden, and M. H. Hitchman, 2022: QBO and ENSO effects on the mean meridional circulation, polar vortex, subtropical westerly jets, and wave patterns during boreal winter. *J. Geophys. Res. Atmos.*, **127**, e2022JD036691, https://doi.org/10.1029/2022JD036691.

Labitzke, K., 1982: On the interannual variability of the middle stratosphere during the northern winters. *J. Meteor. Soc. Japan*, **60**, 124–139, https://doi.org/10.2151/jmsj1965.60.1_124.

Lawrence, Z. D., and Coauthors, 2022: Quantifying stratospheric biases and identifying their potential sources in subseasonal forecast systems. *Wea. Climate Dyn.*, **3**, 977–1001, https://doi.org/10.5194/wcd-3-977-2022.

——, D. Elsbury, A. H. Butler, J. Perlwitz, J. R. Albers, L. M. Ciasto, and E. Ray, 2023: Evaluation of processes related to stratosphere-troposphere coupling in GEFSv12 subseasonal hindcasts. *Mon. Wea. Rev.*, **151**, 1735–1755, https://doi.org/10.1175/MWR-D-22-0283.1.

Liess, S., and M. A. Geller, 2012: On the relationship between QBO and distribution of tropical deep convection. *J. Geophys. Res.*, **117**, 2011JD016317, https://doi.org/10.1029/2011JD016317.

Lim, Y., S.-W. Son, A. G. Marshall, H. H. Hendon, and K.-H. Seo, 2019: Influence of the QBO on MJO prediction skill in the subseasonal-to-seasonal prediction models. *Climate Dyn.*, **53**, 1681–1695, https://doi.org/10.1007/s00382-019-04719-y.

Lin, P., and Y. Ming, 2021: Enhanced climate response to ozone depletion from ozone-circulation coupling. *J. Geophys. Res. Atmos.*, **126**, e2020JD034286, https://doi.org/10.1029/2020JD034286.

Lu, H., T. J. Bracegirdle, T. Phillips, A. Bushell, and L. Gray, 2014: Mechanisms for the Holton-Tan relationship and its decadal variation. *J. Geophys. Res. Atmos.*, **119**, 2811–2830, https://doi.org/10.1002/2013JD021352.

——, M. H. Hitchman, L. J. Gray, J. A. Anstey, and S. M. Osprey, 2020: On the role of Rossby wave breaking in the quasi-biennial modulation of the stratospheric polar vortex during boreal winter. *Quart. J. Roy. Meteor. Soc.*, **146**, 1939–1959, https://doi.org/10.1002/qj.3775.

Ma, T., W. Chen, J. Huangfu, L. Song, and Q. Cai, 2021: The observed influence of the quasi-biennial oscillation in the lower equatorial stratosphere on the East Asian winter monsoon during early boreal winter. *Int. J. Climatol.*, **41**, 6254–6269, https://doi.org/10.1002/joc.7192.

——, ——, X. An, C. I. Garfinkel, and Q. Cai, 2023: Nonlinear effects of the stratospheric quasi-biennial oscillation and ENSO on the North Atlantic winter atmospheric circulation. *J. Geophys. Res. Atmos.*, **128**, e2023JD039537, https://doi.org/10.1029/2023JD039537.

Marsh, D. R., M. J. Mills, D. E. Kinnison, J.-F. Lamarque, N. Calvo, and L. M. Polvani, 2013: Climate change from 1850 to 2005 simulated in CESM1(WACCM). *J. Climate*, **26**, 7372–7391, https://doi.org/10.1175/JCLI-D-12-00558.1.

Martin, Z., C. Orbe, S. Wang, and A. Sobel, 2021a: The MJO–QBO relationship in a GCM with stratospheric nudging. *J. Climate*, **34**, 4603–4624, https://doi.org/10.1175/JCLI-D-20-0636.1.

——, S.-W. Son, A. Butler, H. Hendon, H. Kim, A. Sobel, S. Yoden, and C. Zhang, 2021b: The influence of the quasi-biennial oscillation on the Madden–Julian oscillation. *Nat. Rev. Earth Environ.*, **2**, 477–489, https://doi.org/10.1038/s43017-021-00173-9.

Matthes, K., D. R. Marsh, R. R. Garcia, D. E. Kinnison, F. Sassi, and S. Walters, 2010: Role of the QBO in modulating the influence of the 11 year solar cycle on the atmosphere using constant forcings. *J. Geophys. Res.*, **115**, D18110, https://doi.org/10.1029/2009JD013020.

Mundhenk, B. D., E. A. Barnes, E. D. Maloney, and C. F. Baggett, 2018: Skillful empirical subseasonal prediction of landfalling atmospheric river activity using the Madden–Julian oscillation and quasi-biennial oscillation. *npj Climate Atmos. Sci.*, **1**, 20177, https://doi.org/10.1038/s41612-017-0008-2.

Nardi, K. M., C. F. Baggett, E. A. Barnes, E. D. Maloney, D. S. Harnos, and L. M. Ciasto, 2020: Skillful all-season S2S prediction of U.S. precipitation using the MJO and QBO. *Wea. Forecasting*, **35**, 2179–2198, https://doi.org/10.1175/WAF-D-19-0232.1.

Neale, R. B., J. Richter, S. Park, P. H. Lauritzen, S. J. Vavrus, P. J. Rasch, and M. Zhang, 2013: The mean climate of the Community Atmosphere Model (CAM4) in forced SST and fully coupled experiments. *J. Climate*, **26**, 5150–5168, https://doi.org/10.1175/JCLI-D-12-00236.1.

Noguchi, S., Y. Kuroda, K. Kodera, and S. Watanabe, 2020: Robust enhancement of tropical convective activity by the 2019 Antarctic sudden stratospheric warming. *Geophys. Res. Lett.*, **47**, e2020GL088743, https://doi.org/10.1029/2020GL088743.

O'Reilly, C. H., A. Weisheimer, T. Woollings, L. J. Gray, and D. MacLeod, 2019: The importance of stratospheric initial conditions for winter North Atlantic Oscillation predictability and implications for the signal-to-noise paradox. *Quart. J. Roy. Meteor. Soc.*, **145**, 131–146, https://doi.org/10.1002/qj.3413.

Pang, B., R. Lu, and R. Ren, 2022: Impact of the Scandinavian pattern on long-lived cold surges over the South China Sea. *J. Climate*, **35**, 1773–1785, https://doi.org/10.1175/JCLI-D-21-0607.1.

Park, C.-H., S.-W. Son, Y. Lim, and J. Choi, 2022: Quasi-biennial oscillation-related surface air temperature change over the western North Pacific in late winter. *Int. J. Climatol.*, **42**, 4351–4359, https://doi.org/10.1002/joc.7470.

Plumb, R. A., 1985: On the three-dimensional propagation of stationary waves. *J. Atmos. Sci.*, **42**, 217–229, https://doi.org/10.1175/1520-0469(1985)042<0217:OTTDPO>2.0.CO;2.

——, and R. C. Bell, 1982: A model of the quasi-biennial oscillation on an equatorial beta-plane. *Quart. J. Roy. Meteor. Soc.*, **108**, 335–352, https://doi.org/10.1002/qj.49710845604.

Portal, A., P. Ruggieri, F. M. Palmeiro, J. García-Serrano, D. I. V. Domeisen, and S. Gualdi, 2022: Seasonal prediction of the boreal winter stratosphere. *Climate Dyn.*, **58**, 2109–2130, https://doi.org/10.1007/s00382-021-05787-9.

Rao, J., C. I. Garfinkel, and I. P. White, 2020a: How does the quasi-biennial oscillation affect the boreal winter tropospheric circulation in CMIP5/6 models? *J. Climate*, **33**, 8975–8996, https://doi.org/10.1175/JCLI-D-20-0024.1.

——, ——, and ——, 2020b: Impact of the quasi-biennial oscillation on the northern winter stratospheric polar vortex in CMIP5/6 models. *J. Climate*, **33**, 4787–4813, https://doi.org/10.1175/JCLI-D-19-0663.1.

——, ——, and ——, 2020c: Predicting the downward and surface influence of the February 2018 and January 2019 sudden stratospheric warming events in subseasonal to seasonal (S2S) models. *J. Geophys. Res. Atmos.*, **125**, e2019JD031919, https://doi.org/10.1029/2019JD031919.

——, ——, and ——, 2021: Development of the extratropical response to the stratospheric quasi-biennial oscillation. *J. Climate*, **34**, 7239–7255, https://doi.org/10.1175/JCLI-D-20-0960.1.

Rayner, N. A., D. E. Parker, E. B. Horton, C. K. Folland, L. V. Alexander, D. P. Rowell, E. C. Kent, and A. Kaplan, 2003: Global analyses of sea surface temperature, sea ice, and night marine air temperature since the late nineteenth century. *J. Geophys. Res.*, **108**, 4407, https://doi.org/10.1029/2002JD002670.

Richter, J. H., F. Sassi, R. R. Garcia, K. Matthes, and C. A. Fischer, 2008: Dynamics of the middle atmosphere as simulated by the Whole Atmosphere Community Climate Model, version 3 (WACCM3). *J. Geophys. Res.*, **113**, D08101, https://doi.org/10.1029/2007JD009269.

——, ——, and ——, 2010: Toward a physically based gravity wave source parameterization in a general circulation model. *J. Atmos. Sci.*, **67**, 136–156, https://doi.org/10.1175/2009JAS3112.1.

——, J. A. Anstey, N. Butchart, Y. Kawatani, G. A. Meehl, S. Osprey, and I. R. Simpson, 2020: Progress in simulating the quasi-biennial oscillation in CMIP models. *J. Geophys. Res. Atmos.*, **125**, e2019JD032362, https://doi.org/10.1029/2019JD032362.

Sakaeda, N., J. Dias, and G. N. Kiladis, 2020: The unique characteristics and potential mechanisms of the MJO-QBO relationship. *J. Geophys. Res. Atmos.*, **125**, e2020JD033196, https://doi.org/10.1029/2020JD033196.

Scaife, A. A., and Coauthors, 2017: Tropical rainfall, Rossby waves and regional winter climate predictions. *Quart. J. Roy. Meteor. Soc.*, **143** (702), 1–11, https://doi.org/10.1002/qj.2910.

Sena, A. C. T., Y. Peings, and G. Magnusdottir, 2022: Effect of the quasi-biennial oscillation on the Madden Julian oscillation teleconnections in the Southern Hemisphere. *Geophys. Res. Lett.*, **49**, e2021GL096105, https://doi.org/10.1029/2021GL096105.

Serva, F., and Coauthors, 2022: The impact of the QBO on the region of the tropical tropopause in QBOi models: Present-day simulations. *Quart. J. Roy. Meteor. Soc.*, **148**, 1945–1964, https://doi.org/10.1002/qj.4287.

Silverman, V., N. Harnik, K. Matthes, S. W. Lubis, and S. Wahl, 2018: Radiative effects of ozone waves on the Northern Hemisphere polar vortex and its modulation by the QBO. *Atmos. Chem. Phys.*, **18**, 6637–6659, https://doi.org/10.5194/acp-18-6637-2018.

——, S. W. Lubis, N. Harnik, and K. Matthes, 2021: A synoptic view of the onset of the midlatitude QBO signal. *J. Atmos. Sci.*, **78**, 3759–3780, https://doi.org/10.1175/JAS-D-20-0387.1.

Smith, K. L., R. R. Neely, D. R. Marsh, and L. M. Polvani, 2014: The Specified Chemistry Whole Atmosphere Community Climate Model (SC-WACCM). *J. Adv. Model. Earth Syst.*, **6**, 883–901, https://doi.org/10.1002/2014MS000346.

Son, S.-W., Y. Lim, C. Yoo, H. H. Hendon, and J. Kim, 2017: Stratospheric control of the Madden–Julian oscillation. *J. Climate*, **30**, 1909–1922, https://doi.org/10.1175/JCLI-D-16-0620.1.

Tegtmeier, S., J. Anstey, S. Davis, I. Ivanciu, Y. Jia, D. McPhee, and R. Pilch Kedzierski, 2020: Zonal asymmetry of the QBO temperature signal in the tropical tropopause region. *Geophys. Res. Lett.*, **47**, e2020GL089533, https://doi.org/10.1029/2020GL089533.

Wang, J., H.-M. Kim, and E. K. M. Chang, 2018: Interannual modulation of Northern Hemisphere winter storm tracks by

the QBO. *Geophys. Res. Lett.*, **45**, 2786–2794, https://doi.org/10.1002/2017GL076929.

Watson, P. A. G., and L. J. Gray, 2014: How does the quasi-biennial oscillation affect the stratospheric polar vortex? *J. Atmos. Sci.*, **71**, 391–409, https://doi.org/10.1175/JAS-D-13-096.1.

Wei, K., W. Chen, and R. Huang, 2007: Association of tropical Pacific sea surface temperatures with the stratospheric Holton-Tan oscillation in the Northern Hemisphere winter. *Geophys. Res. Lett.*, **34**, 2007GL030478, https://doi.org/10.1029/2007GL030478.

White, I. P., H. Lu, N. J. Mitchell, and T. Phillips, 2015: Dynamical response to the QBO in the northern winter stratosphere: Signatures in wave forcing and eddy fluxes of potential vorticity. *J. Atmos. Sci.*, **72**, 4487–4507, https://doi.org/10.1175/JAS-D-14-0358.1.

——, ——, ——, and ——, 2016: Seasonal evolution of the QBO-induced wave forcing and circulation anomalies in the northern winter stratosphere. *J. Geophys. Res. Atmos.*, **121**, 10 411–10 431, https://doi.org/10.1002/2015JD024507.

Yamashita, Y., H. Akiyoshi, and M. Takahashi, 2011: Dynamical response in the Northern Hemisphere midlatitude and high-latitude winter to the QBO simulated by CCSR/NIES CCM. *J. Geophys. Res.*, **116**, D06118, https://doi.org/10.1029/2010JD015016.

Yamazaki, K., T. Nakamura, J. Ukita, and K. Hoshi, 2020: A tropospheric pathway of the stratospheric quasi-biennial oscillation (QBO) impact on the boreal winter polar vortex. *Atmos. Chem. Phys.*, **20**, 5111–5127, https://doi.org/10.5194/acp-20-5111-2020.

Zhang, J., F. Xie, Z. Ma, C. Zhang, M. Xu, T. Wang, and R. Zhang, 2019: Seasonal evolution of the quasi-biennial oscillation impact on the Northern Hemisphere polar vortex in winter. *J. Geophys. Res. Atmos.*, **124**, 12 568–12 586, https://doi.org/10.1029/2019JD030966.

Zuo, J., F. Xie, L. Yang, C. Sun, L. Wang, and R. Zhang, 2022: Modulation by the QBO of the relationship between the NAO and Northeast China temperature in late winter. *J. Climate*, **35**, 7995–8011, https://doi.org/10.1175/JCLI-D-22-0353.1.